Density Functional Study of Interactions between Fluorinated Cyclohexanes and Arenes

by **Rodrigo A. Cormanich**[a][b], **Alastair Durie**[a], **Ragnar Bjornsson**[c], **Roberto Rittner**[b], **David O'Hagan***[a], and **Michael Bühl***[a]

[a]) EastChem School of Chemistry and Centre of Magnetic Resonance, University of St Andrews, North Haugh, St Andrews, Fife, KY16 9ST, UK (phone: +44-1334-467171; fax: +44-1334-463800; e-mail: mb105@st-andrews.ac.uk; do1@st-andrews.ac.uk)

[b]) Chemistry Institute, University of Campinas, Campinas, SP, 13083-970, Brazil (phone: +55-19-35213150; fax: +55-19-35213023)

[c]) MPI for Chemical Energy Conversion, Stiftstrasse 34–36, D-45470 Mülheim an der Ruhr

^{1}H-NMR Chemical shifts of all-*syn*-1,2,4,5-tetrafluorocyclohexane (**1**), all-*syn*-1,2,3,4-tetrafluorocyclohexane (**2**), and their complexes with benzene are calculated at the BHandH/6-311+G(2d,p) level. The observed shielding of certain resonances on going from CD_2Cl_2 to (D_8)toluene solution is qualitatively reproduced in these model calculations, in particular when standard B3LYP/def2-TZVP optimised geometries are employed. The results are interpreted with the quantum theory of atoms in molecules (QTAIM) and non-covalent interactions (NCI) methods, and they indicate that aromatic molecules bind strongly (1.6 kcal mol^{-1}) to the 'positive face' of these molecules. The level of theory is validated for the new compound all-*syn*-1,2,4,5-tetrafluoro-3-phenylcyclohexane (**3**), where a recently developed QM/MM protocol for optimisation of molecular crystals afforded excellent agreement between the B3LYP/def2-TZVP structure and that observed in the solid.

Introduction. – Fluorine compounds have been widely used in many fields, especially in medicinal and material sciences. The inclusion of F-atoms and/or fluorinated groups provide new and unusual molecular properties, which indeed can be used to obtain more active and selective drugs and materials with improved efficiencies [1][2]. In this context, *Durie et al.* reported the synthesis of the all-*syn*-1,2,4,5-tetrafluorocyclohexane (**1**) and the all-*syn*-1,2,3,4-tetrafluorocyclohexane (**2**) [3][4], which were shown to have high polarity and low viscosity, and, hence, are potentially new candidates to be used as liquid crystal materials. Some ^{1}H-NMR resonances of **1** and **2** showed unusually strong upfield shifts on going from CD_2Cl_2 to (D_8)toluene solution, which were not fully rationalised at the time [3]. We now report theoretical calculations for **1** and **2** using simple solvation models to highlight the specific interactions with aromatic solvent molecules which give rise to these unusual upfield shifts.

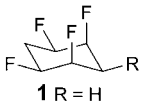

1 R = H
3 R = Ph

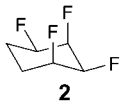

2

A model for the interaction between the fluorinated cyclohexane moieties and aromatic groups was provided by the recent synthesis and characterisation of all-*syn*-1,2,4,5-tetrafluoro-3-phenylcyclohexane (**3**) [5]. Using a suitable computational protocol, we now report on the effect of intermolecular packing on the ^{1}H chemical shifts in **3**, which is of interest in relation with the above mentioned solvent shifts in **1** (and **2**).

Results and Discussion. – The experimental ^{1}H-NMR chemical shifts of **1** and **2**, recorded in CD_2Cl_2 and (D_8)toluene, of all-*syn*-1,2,4,5-tetrafluorocyclohexane (**1**) and all-*syn*-1,2,3,4-tetrafluorocyclohexane (**2**) are compiled in *Table 1*. The shielding of the ^{1}H resonances on going from CD_2Cl_2 to (D_8)toluene is a manifestation of the well-known aromatic solvent-induced shift (ASIS) [6], albeit of exceptional magnitude, as individual chemical-shift changes reach up to $\Delta\delta$ of 1.7 ppm. To rationalise these findings, we performed density functional theory (DFT) calculations for **1** and **2** (*Fig. 1*), as well as for their complexes with a single benzene molecule (as a model for toluene)[1]) attached at the 'positive face', *i.e.*, on the opposite molecular side of the axial F-atoms (*Fig. 2*).

Both **1** and **2** have large dipole moments and highly polarised charge distributions that are very negative at the molecular face containing the F-atoms ('negative face') and positive at the opposite face ('positive face', see electrostatic potentials (ESPs) in *Fig. 1*). The electron-rich aromatic solvent molecules bind preferentially to the positive faces (with a binding energy of *ca.* 1.6 kcal mol^{-1} for both **1** and **2** at the B3LYP/def2-TZVP [7] level). This result is confirmed by the molecular graphs obtained from the quantum theory of atoms in molecules (QTAIM) [8] and an analysis based on the recently developed non-covalent interactions (NCI) method [9] (*Fig. 2*). The latter has been developed from the former to overcome ambiguities in the classification of weak

Table 1. *Experimental and Theoretical* (BHandH/6-311 + G(2d,p))[a]) *^{1}H-NMR Chemical Shifts* (δ in ppm) *for Compounds* **1** *and* **2** (for atom numbering, see *Fig. 1*)

H-Atom	**1** (exper.)			**1** (theoretical)			**2** (exper.)			**2** (theoretical)		
	$\delta(CD_2Cl_2)$	δ(toluene)	$\Delta\delta$	free **1**	**1**·C_6H_6	$\Delta\delta$	$\delta(CD_2Cl_2)$	δ(toluene)	$\Delta\delta$	free **2**	**2**·C_6H_6	$\Delta\delta$
H7	4.94	4.06	−0.88	4.88	4.48	−0.40	5.26	4.60	−0.66	5.28	4.88	−0.40
H8	1.63	−0.06	−1.69	1.23	0.37	−0.86	4.45	2.74	−1.71	4.04	2.77	−1.27
H9	2.46	1.74	−0.72	2.63	2.17	−0.46	na[b])	na	na	na	na	na
H10	4.94	4.06	−0.88	4.88	4.48	−0.40	5.04	4.12	−0.92	4.95	4.46	−0.49
H11	4.53	3.22	−1.31	4.30	3.55	−0.75	4.57	3.30	−1.27	4.30	3.58	−0.72
H12	2.37	1.84	−0.53	2.28	1.89	−0.39	1.93	2.16	0.23	1.74	1.39	−0.35
H13	2.61	2.76	+0.15	2.87	2.55	−0.32	1.47	0.05	−1.42	2.47	2.16	−0.31
H14	4.53	3.22	−1.31	4.30	3.55	−0.75	2.10	1.16	−0.94	1.17	0.45	−0.72
H17	na	na	na	na	na	na	2.28	1.32	−0.96	2.24	1.84	−0.40

[a]) B3LYP/def2-TZVP Geometries employed. [b]) Not available.

[1]) Benzene was used as model because it has very similar electronic properties as toluene, but lacks the conformational complexity in an adduct (*i.e.*, relative positions of the additional Me group and the F-atoms in the cyclohexane).

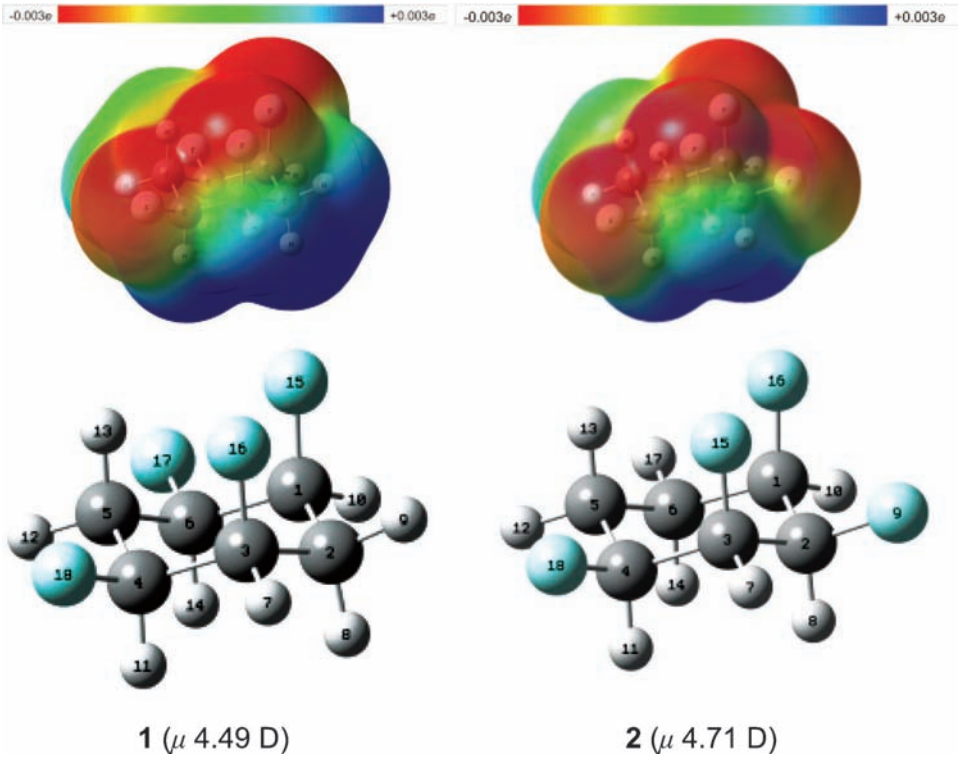

Fig. 1. *Optimised structures, electrostatic potentials* (ESPs), *and dipole moments of* **1** *and* **2** (B3LYP/def2-TZVP). ESPs are plotted on a color scale from -0.03 a.u. (*red*) to $+0.03$ a.u. (*blue*) and mapped onto an isodensity surface ($\rho = 4 \cdot 10^{-4}$ a.u.).

interatomic interactions as attractive or repulsive, which is achieved by performing the topological analysis of the reduced density gradient (RDG) instead of the electron density (ρ) itself.

Both methods indicate not only formation of $\pi \cdots$ H–C intermolecular interactions between the cyclohexane and benzene moieties (for details of their QTAIM characterisation, see Table S1 in the *Electronic Supporting Information* (*ESI*)), but also intramolecular F$\cdots$F interactions within **1** and **2** (also for the free molecules; not shown). Such interactions have attracted much interest and controversy in the literature [10][11]. According to our NCI analysis (*Fig. 3*), these interactions emerge formally as attractive.

Solute–solvent interaction potentials were obtained through relaxed scans of salient distances between aliphatic H- and aromatic C-atoms in steps of 0.03 Å at the B3LYP and B97-D levels (B3LYP results shown in *Fig. 4*). The B97-D level was chosen in addition to the popular B3LYP functional, because it was suspected that dispersion interactions would be very important. Indeed, on going from B3LYP to B97-D, the minimum deepens considerably (from *ca.* -1.6 kcal/mol (see *Fig. 4*) to *ca.* -6 kcal/mol (see Fig. S1)) and is shifted to shorter distances (from *ca.* 3.1–3.2 Å to *ca.*

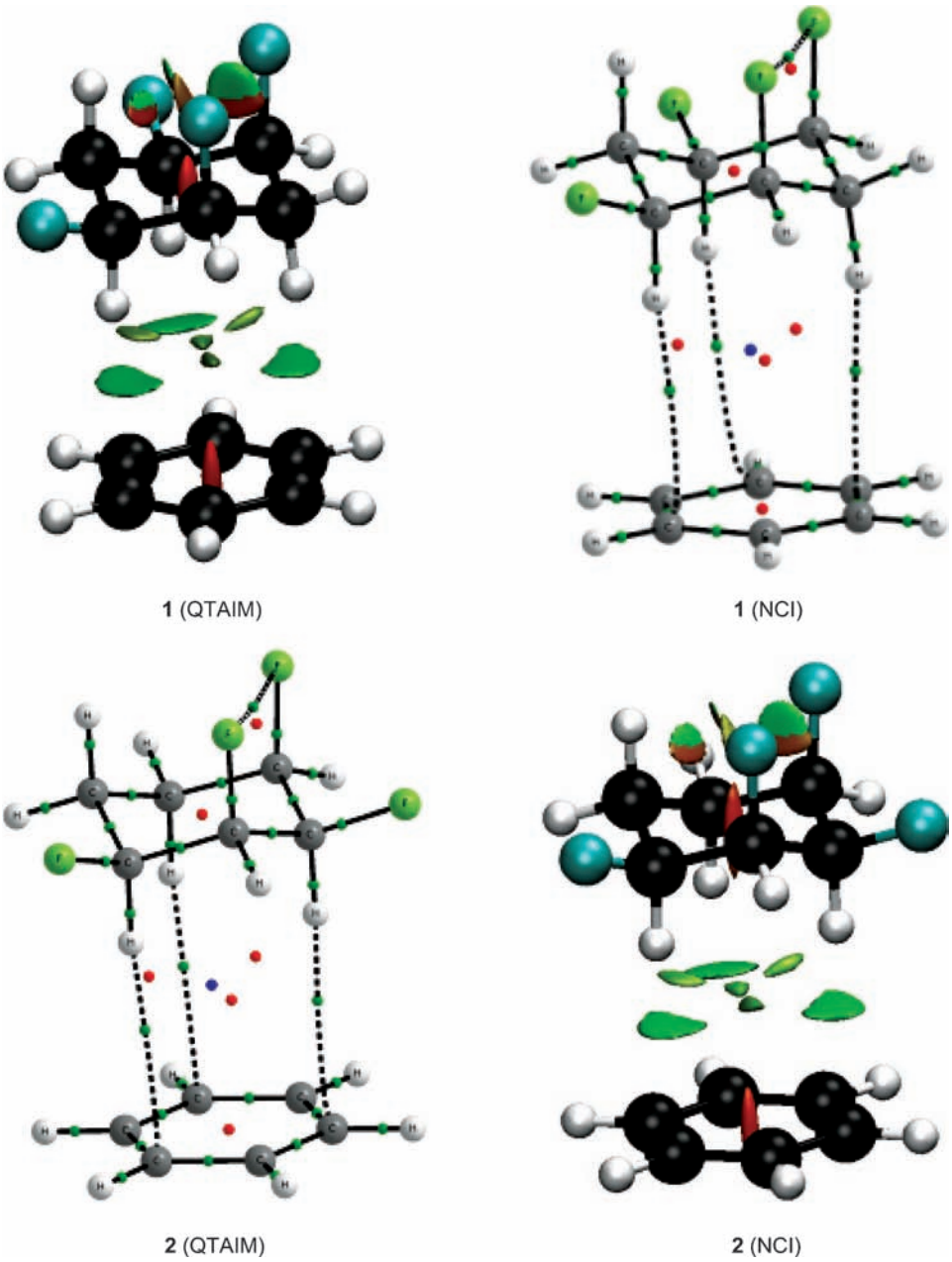

Fig. 2. *QTAIM and NCI molecular graphs obtained from the B3LYP/def2-TZVP electron density.* Green, red, and blue points in the QTAIM graphs represent bond critical points (BCPs), ring critical points (RCPs), and cage critical points (CCPs), respectively. NCI Surfaces are *green* for attractive *Van der Waals* interactions and *red* for internal ring electron-density depletion/repulsion (analogous to ring-critical points in QTAIM). NCI Plots were obtained with RDG of 0.6 and blue–green–red scale ranging from – 0.04 to 0.04 au.

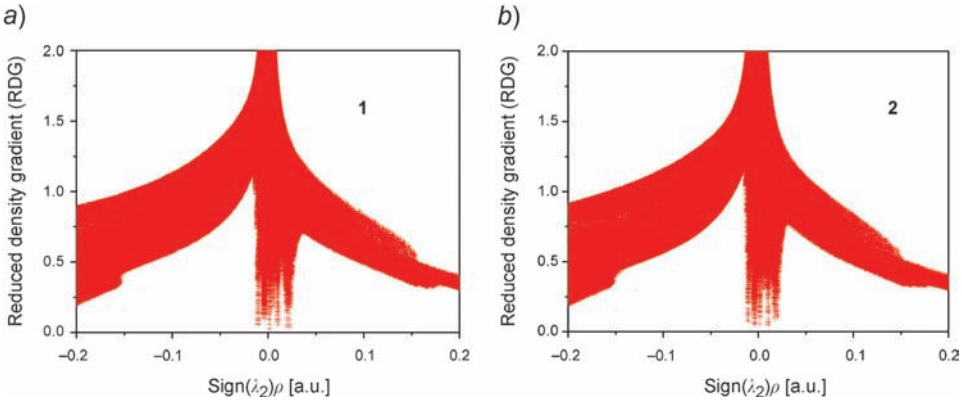

Fig. 3. *Plot of the reduced density grandient* (RDG) vs. *sign(λ_2)ρ for* a) *compound* **1** *and* b) *compound* **2** (sign(λ_2) means the sign (positive or negative) of second eigenvalue λ_2 of the *Laplacian* of the electron density ρ). Downward peaks at negative sign(λ_2)ρ values indicate attractive non-covalent interactions in the regions between the axial F-atoms, downward peaks at positive sign(λ_2)ρ values indicate ring/cage critical point regions.

2.6–2.7 Å). Essentially, the same results are obtained when the empirical dispersion corrections [12][13] are added as single points to the structures of the B3LYP scan (see B3LYP-D and B3LYP-D3 data in Fig. S1).

The ^{1}H-NMR chemical shifts were calculated both for free molecules **1** and **2**, and for their complexes with benzene, using B3LYP and B97-D geometries. It was expected that the difference between the isolated molecules and the benzene complexes could be related to the observed solvent shifts on going from CH_2Cl_2 to toluene. In fact, the results for both sets of structures (B3LYP and B97-D) follow the observed trends reasonably well in a qualitative sense, in particular for compound **1**, where the relative order of shifts of the individual signals is well reproduced (see filled circles in the plot in *Fig. 5*). Interestingly, the shifts calculated for the B3LYP structures afforded a slightly better qualitative agreement with experiment (compare the $\Delta\delta$ values in *Table 1*) than those calculated for the tighter B97-D minima (Tables S2–S5). For the latter, individual deviations between modeled and observed solvent shifts can reach up to *ca.* 2 ppm (*e.g.*, for H8 in compound **2**; Table S5).

As a consequence of such complexation of **1** and **2** with benzene, the benzene ring current [14] effectively shields those H-atoms in its 'shielding cone' perpendicular to the molecular plane. It is thus the H-atoms lying in the positive molecular ESP area, *i.e.*, atoms H8, H11, and H14, which experience the highest shielding effect, since these interact strongly with the solvent and, hence, are closer to the shielding cone of the aromatic rings. As mentioned above, when dispersion corrections are included in calculating the alkane–arene interaction energies (either *via* B3LYP-D3 single points or at the B97-D level), the minima in *Fig. 4* deepen and shift to lower distances (Fig. S1). The chemical shifts are sensitive to this distance and deteriorate noticeably for such dispersion-corrected minima. Apparently, B3LYP (which describes the leading electrostatic contributions correctly) affords reasonable models for averaged (rather than equilibrium) structures in these cases.

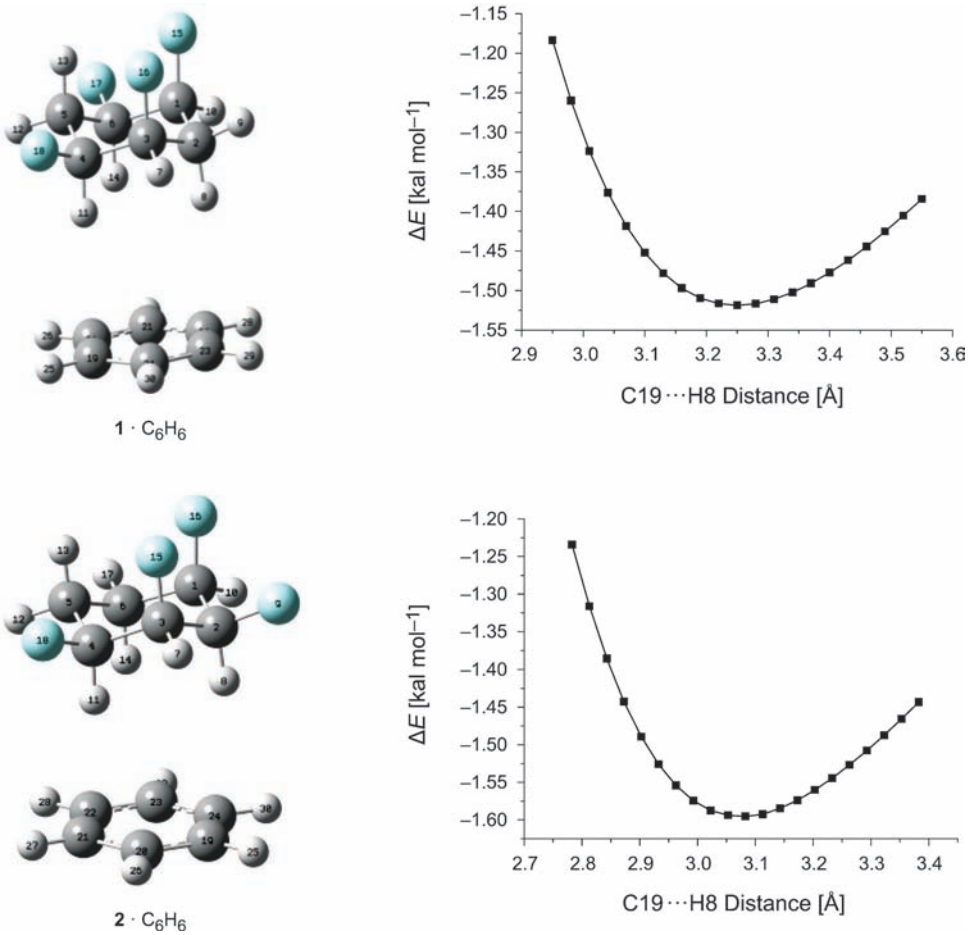

Fig. 4. *Optimised complexes of* **1** *and* **2** *with benzene and interaction energies at the B3LYP/def2-TZVP level*

For a more quantitative description, one would have to include more solvent molecules and model their time-averaged effect on the solute shifts, *e.g.*, by way of molecular dynamics simulations. That our simple theoretical model can already capture a large part of the observed effect can be taken as evidence for a predominance of solute–solvent complexes like those in *Fig. 2* in the dynamic ensemble in solution. Note that the observed pattern in the solvent shifts is due to ring-current effects in such solute–solvent complexes, rather than to bulk solvation effects. This is demonstrated by repeating the NMR calculations for the monomer immersed in a polarisable continuum model (PCM) of benzene. Relative to the gas-phase results, the obtained NMR chemical shifts are deshielded rather uniformly without distinguishing H-atoms from either face (by *ca.* 0.3 and 0.2 ppm for **1** and **2**, resp.; see Table S6).

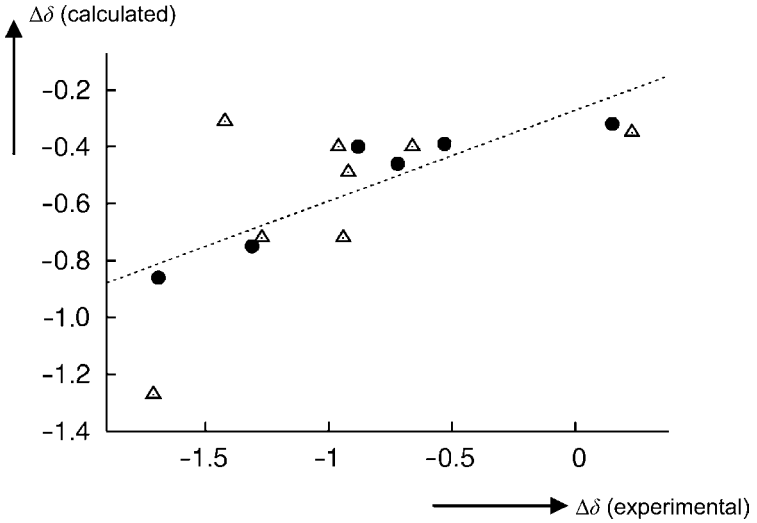

Fig. 5. *Plot of calculated shifts in ^{1}H-NMR resonances upon complex formation with benzene* vs. *observed shift differences on going from CH_2Cl_2 to toluene solutions* (in ppm). ●: compound **1**, △: compound **2**.

Recently, the synthesis and structure of all-*syn*-1,2,4,5-tetrafluoro-3-phenylcyclohexane (**3**) were reported [5]. This compound is an analog of **1**, which was also proposed as a new structural motif for liquid crystals. This compound turned out to be a good model to analyze the complexation of **1** with aromatic groups, since it was possible to obtain the X-ray structure for **3**, and it was observed that the Ph groups interact with the 'positive face' of cyclohexane rings in neighboring molecules in almost the same geometry we have obtained for **1** (*Fig. 6,c*).

Comparing the observed intermolecular cyclohexane-arene distance in **3** (C ··· H *ca.* 3.46 Å) with that in **1** · C_6H_6, the B3LYP-optimised values for the latter are closer (*ca.* 3.25 Å; left part of *Fig. 2*) than the B97-D data (*ca.* 2.71 Å; left part in Fig. S1). To probe whether the apparent good performance of B3LYP holds for the intermolecular interactions in **3** as well, we optimised the full molecular crystal employing the recently developed QM/MM protocol by *Bjornsson* and *Bühl* (see *Computational Details*) [15] together with a variety of standard functionals with and without explicit dispersion corrections. Key interatomic distances obtained by each method and from experiment are shown in Tables S7 and S8 in the *ESI*. Compared to pristine **1** · C_6H_6 in the gas phase, inclusion of dispersion corrections has a much smaller effect on the intermolecular distances in solid **3**. For example, on going from B3LYP/def2-TZVP to B3LYP-D3/def2-TZVP, most intermolecular distances between the cyclohexane and the neighboring Ph moieties decrease slightly, by less than 0.03 Å (see C ··· C distances in Table S8), *i.e.*, by much less than for the pristine benzene complexes **1** · C_6H_6 and **2** · C_6H_6 discussed above. Overall, the B3LYP/def2-TZVP level performs best in reproducing the structure in the solid, as judged by the root-mean-square deviation (RMSD) between the optimised and observed coordinates of all C- and F-atoms in the trimeric QM region (*ca.* 0.04 Å; *Fig. 7,a*). All other level/basis-set combinations

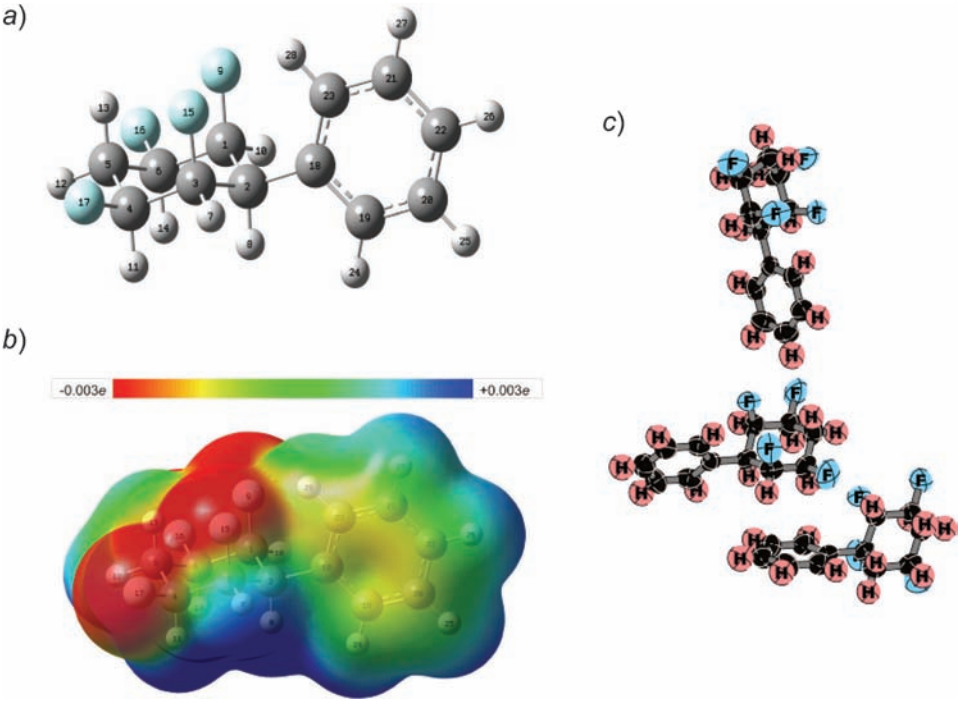

Fig. 6. a) *B3LYP/def2-TZVP-Optimised structure of compound* **3**, b) *its calculated ESP, showing the 'positive face'* (lower molecular part) *and 'negative face'* (upper molecular part, see caption of *Fig. 1* for details), *and* c) *experimental X-ray structure showing the interaction of a Ph group located in the lower molecule with the 'positive face' of the cyclohexane ring of the central molecule in an almost parallel arrangement.* Note the interaction between the 'negative face' of the central cyclohexane ring with another Ph group from the upper molecule in a perpendicular arrangement.

(including dispersion-corrected functionals) afford slightly higher RMSDs, up to *ca.* 0.08 Å (Table S8).

The effect of the crystal environment on the relative orientation of the molecular interactions can be probed by relaxing a section, *e.g.*, the trimer shown in *Fig. 7,a*, in the gas phase. As can be seen in *Fig. 7,b*, the B3LYP/def2-TZVP minimum of this trimer in the gas phase is noticeably distorted from that in the crystal.

^{1}H-NMR Chemical shifts for **3** were obtained at the BHandH/6-311 + G(2d,p) level for a single isolated molecule and for the central molecule embedded in the trimer (B3LYP/def2-TZVP QM/MM geometries; *Table 2*). The data for the trimer are in good agreement with those of compound **1** complexed with benzene (compare values in *Tables 1* and *2*). Also, the computed trends upon complex formation for compound **3** are similar to that obtained for compound **1**. The ^{1}H-NMR chemical-shift calculations for monomeric **3** also agree with the experimental values obtained in $CDCl_3$ (*Table 2*). These findings confirm that, as expected, the intermolecular contacts seen in the crystal are all lost upon dissolution in $CDCl_3$ (*i.e.*, no smaller aggregates are preserved). The $\Delta\delta$ values between monomer and complex compiled in *Table 2* can serve as predictions

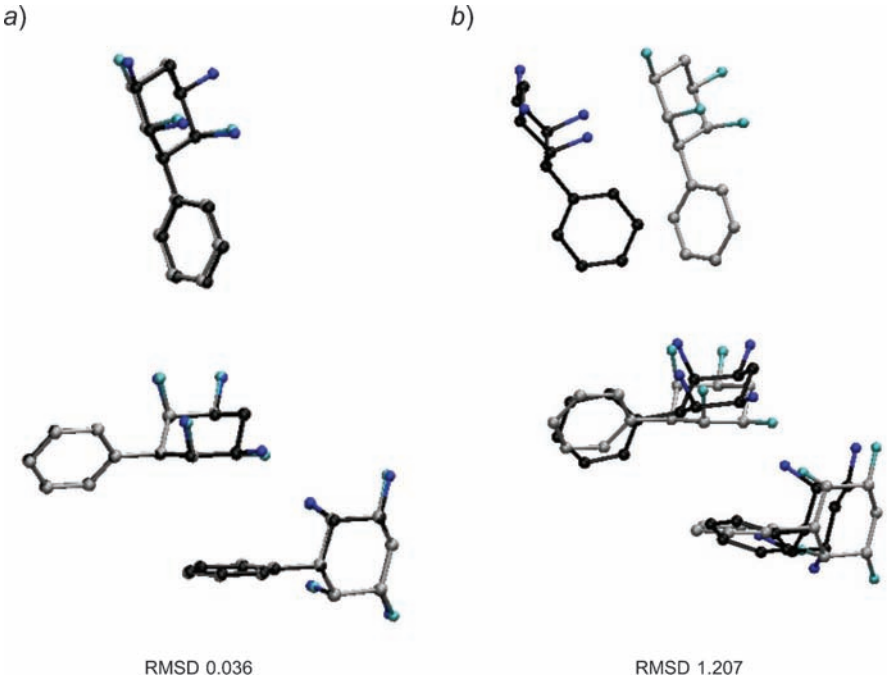

Fig. 7. *Superposition of a section of the experimental crystal structure of compound* **3** (grey/light blue) *with* a) *the same section from the QM/MM-optimised crystal* (black/dark blue) *and* b) *gas-phase calculated geometries* (B3LYP/def2-TZVP; black/dark blue)*, including root-mean-square deviation* (RMSD, in Å) *between both.*

Table 2. *Theoretical* (BHandH/6-311 + G(2d,p)) *^{1}H-NMR Isotropic Magnetic Shieldings* (σ) *and Chemical Shifts* (δ in ppm) *for Free Monomeric* **3**, *and for the Central Molecule in the QM Trimer within the QM/MM-Optimised Crystal of* **3** (B3LYP/def2-TZVP)*, together with Experimental Data in Solution* (for atom numbering, see *Fig. 6*)

H-Atom	σ(monomer)	δ(monomer)[a])	σ(complex)	δ(complex)[a])	$\Delta\delta$	$\delta(CDCl_3)$ Exper.
H7, H10	26.04	5.58	26.44	5.18	– 0.40	5.05
H8	29.00	2.62	29.16	2.46	– 0.16	2.63
H11, H14	26.79	4.83	28.65	2.97	– 1.86	4.62
H12	28.80	2.82	29.31	2.31	– 0.51	2.81
H13	28.13	3.49	29.44	2.18	– 1.31	2.51

[a]) $\delta = \sigma_{TMS}$ (31.62 ppm) – σ_H.

for the expected solution-to-solid shifts once solid-state NMR studies of compound **3** become available.

Conclusions. – Overall, simple theoretical models can rationalise the experimentally observed chemical-shift values in toluene solution for the compounds **1** and **2**. The

leading contribution is indicated to arise from close contact between an aromatic ring from the solvent and the 'positive face' of the cyclohexane ring opposite to the F-substituents. The qualitative trends are reproduced for simple complexes between **1** or **2**, and a single benzene molecule at the B3LYP level, *i.e.*, even without inclusion of dispersion corrections. This level has also been validated using a recently developed QM/MM protocol for the optimisation of molecular crystals, where excellent agreement was found between the B3LYP-computed and the observed crystal structure for the new compound **3**, which is governed by such intermolecular cyclohexane ··· arene interactions. The attractive nature of these interactions is also apparent in a recently proposed analysis based on the Quantum Theory of Atoms in Molecules (QTAIM) approach, namely the Non-Covalent Interactions (NCI) method.

Computational Details. – Geometries were fully optimised at the B3LYP/def2-TZVP and B97-D/def2-TZVP levels, resp., and magnetic shieldings were evaluated at the BHandH/6-311 + G(2d,p) level (Tables S2 – S5 in the ESI) by using Gaussian 09 Revision A.02 program [16]. ^{1}H-NMR Magnetic shieldings were converted into relative shifts δ using the ^{1}H magnetic shielding in TMS computed at the same respective levels (31.62 and 31.38 ppm for B3LYP and B97-D geometries, resp.). Selected calculations were also performed using a polarisable continuum model in the NMR calculation (in its integral equation formalism variant, IEF-PCM) [17], using the parameters of benzene (dielectric constant, 2.27). The QTAIM and NCI methods were carried out by using the AIMALL [18] and NCIPLOT [19] programs, resp., on the B3LYP/def2-TZVP-obtained electron densities.

The QM/MM protocol [15] for optimising the crystal structure of **3** was carried out by using the Chemshell [20] program linked to ORCA [21] program and adapted as follows: a cluster with a radius of 42 Å (containing 33,880 atoms/1210 molecules) was taken from the exper. crystal structure. Atomic charges from natural population analysis (NPA) for a free molecule **3** were obtained at a variety of DFT levels (different functional were used in the present work; see below) and were assigned to all other molecules of the built cluster. Surface charges were added on the boundaries of the cluster to emulate the remaining, infinite periodic system. The NPA charges were then refined self-consistently in a series of QM/MM single-point calculations for a single molecule **3** electrostatically embedded in the surrounding MM point charges (cluster and the cluster boundary charges were updated in each cycle self-consistently, until the charges changed by less than 0.0001 au). Assigning *Van der Waals* parameters from the UFF force field to all atoms in the cluster (to derive 6 – 12 *Lennard-Jones* potentials for all atom pairs), the NPA charges were refined again through a series of QM/MM geometry optimisations where only the central molecule was included in the QM region, while all other MM molecules were kept frozen. Finally, the QM region was enlarged to encompass the central molecule and two neighboring molecules (affording a trimer as shown in *Fig. 6,c*), and QM/MM optimisations were carried out using the self-consistent charges determined previously. These calculations used BP86, B3LYP, revPBE [22], and PW6B95 [23] functionals with and without *Grimme* dispersion corrections (DFT-D3) [12][13], and with the def2-SVP and def2-TZVP basis sets [7]. ^{1}H-NMR Chemical shifts were calculated at the BHandH/6-311 + G(2d,p) level for the B3LYP/def2TZVP-optimised trimer, embedded in the array of MM point charges (reported for the central molecule only). Relaxation of the QM region containing the trimer in the gas phase started from the QM/MM-optimised coordinates using ORCA.

The authors thank a Grant # 2012/03933-5, *São Paulo Research Foundation* (*FAPESP*), for providing financial support for this research, for a scholarship (to *R.A.C.* #2011/01170-1, FAPESP). CNPq is also gratefully acknowledged for a fellowship (to *R.R*) and a studentship (to *R.A.C.*). We thank the *Royal Society (Wolfson Merit Award for D.O'H.)* and EaStCHEM (support for *M.B.* and access to a computing facility maintained by *H. Früchtl*).

REFERENCES

[1] D. O' Hagan, *Chem. Soc. Rev.* **2008**, *37*, 308.
[2] R. Berger, G. Resnati, P. Metrangolo, E. Weberd, J. Hulliger, *Chem. Soc. Rev.* **2011**, *40*, 3496.
[3] A. J. Durie, A. M. Z. Alexandra, T. Lebl, P. Kirsch, D. O' Hagan, *Chem. Commun.* **2011**, *47*, 8265.
[4] A. J. Durie, A. M. Z. Slwein, T. Lebl, P. Kirsch, D. O' Hagan, *Chem. Commun.* **2012**, *48*, 9643.
[5] A. J. Durie, T. Fujiwara, R. Cormanich, M. Bühl, A. M. Z. Slawin, D. O' Hagan, *Chem. – Eur. J.* **2014**, *20*, 6259.
[6] E. M. Engler, P. Laszlo, *J. Am. Chem. Soc.* **1971**, *93*, 1317.
[7] F. Weigend, R. Ahlrichs, *Phys. Chem. Chem. Phys.* **2005**, *7*, 3297.
[8] R. F. W. Bader, 'Atoms in Molecules, A Quantum Theory', Clarendon, Oxford, 1990.
[9] E. Johnson, S. Keinan, P. Mori-Sánchez, J. Contreras-García, A. Cohen, W. Yang, *J. Am. Chem. Soc.* **2010**, *132*, 6498.
[10] T. V. Rybalova, I. Y. Bagryanskaya, *J. Struct. Chem.* **2009**, *50*, 741.
[11] R. M. Osuna, V. Hernández, J. T. L. Navarrete, E. D'Oria, J. J. Novoa, *Theor. Chem. Acc.* **2011**, *128*, 541.
[12] S. Grimme, S. Ehrlich, L. Goerigk, *J. Comput. Chem.* **2011**, *32*, 1456.
[13] S. Grimme, J. Antony, S. Ehrlich, H. Krieg, *J. Chem. Phys.* **2010**, *132*, 154104.
[14] P. Lazzeretti, *Prog. NMR Spectr.* **2000**, *36*, 1.
[15] R. Bjornsson, M. Bühl, *J. Chem. Theory Comput.* **2012**, *8*, 498.
[16] Gaussian 09, Revision A.02, M. J. Frisch, G. W. Trucks, H. B. Schlegel, G. E. Scuseria, M. A. Robb, J. R. Cheeseman, G. Scalmani, V. Barone, B. Mennucci, G. A. Petersson, H. Nakatsuji, M. Caricato, X. Li, H. P. Hratchian, A. F. Izmaylov, J. Bloino, G. Zheng, J. L. Sonnenberg, M. Hada, M. Ehara, K. Toyota, R. Fukuda, J. Hasegawa, M. Ishida, T. Nakajima, Y. Honda, O. Kitao, H. Nakai, T. Vreven, J. A. Montgomery Jr., J. E. Peralta, F. Ogliaro, M. Bearpark, J. J. Heyd, E. Brothers, K. N. Kudin, V. N. Staroverov, R. Kobayashi, J. Normand, K. Raghavachari, A. Rendell, J. C. Burant, S. S. Iyengar, J. Tomasi, M. Cossi, N. Rega, J. M. Millam, M. Klene, J. E. Knox, J. B. Cross, V. Bakken, C. Adamo, J. Jaramillo, R. Gomperts, R. E. Stratmann, O. Yazyev, A. J. Austin, R. Cammi, C. Pomelli, J. W. Ochterski, R. L. Martin, K. Morokuma, V. G. Zakrzewski, G. A. Voth, P. Salvador, J. J. Dannenberg, S. Dapprich, A. D. Daniels, O. Farkas, J. B. Foresman, J. V. Ortiz, J. Cioslowski, and D. J. Fox, Gaussian, Inc., Wallingford CT, 2009.
[17] G. Scalmani, M. J. Frisch, *J. Chem. Phys.* **2010**, *132*, 114110.
[18] A. K. Todd, AIMAll (Version 13.05.06), 2013 (aim.tkgristmill.com).
[19] J. Contreras-García, E. R. Johnson, S. Keinan, R. Chaudret, J.-P. Piquemal, D. N. Beratan, W. Yang, *J. Chem. Theor. Comput.* **2011**, *7*, 625.
[20] a) ChemShell, a Computational Chemistry Shell, see www.chemshell.org; b) S. Metz, J. Kästner, A. A. Sokol, T. W. Keal, P. Sherwood, *WIREs Comput. Mol. Sci.* **2014**, *4*, 101.
[21] F. Neese, ORCA, University of Bonn, Bonn, Germany, 2010, http://www.thch.uni-bonn.de/tc/orca.
[22] Y. Zhang, W. Yang, *Phys. Rev. Lett.* **1998**, *80*, 890.
[23] Y. Zhao, D. G. Truhlar, *J. Phys. Chem. A* **2005**, *109*, 5656.

Received February 12, 2014